



Pipeline Corrosion Monitoring by Fiber Optic Distributed Strain and Temperature Sensors

Lufan Zou* and Omur Sezerman

OZ Optics Ltd.

219 Westbrook Road, Ottawa, ON, Canada K0A 1L0

Winston Revie

CANMET Materials Technology Laboratory, Natural Resources Canada

Ottawa, ON, Canada

ABSTRACT

Brillouin-scattering-based fiber optic distributed strain and temperature sensors (DSTS) has been applied to measure the longitudinal and hoop strain in an internally pressurized 1.8 m long end-capped steel pipe with wall thinning defects. The pre-embedded defects, which constitute 50–60% of inner wall thickness to simulate the structural degradation by corrosion in pipes, are discriminated by use of the corresponding strain measurements in the axial and hoop directions along the pipe with our distributed strain and temperature sensor system using 10 cm spatial resolution. The locations of structural indentations are found and distinguished by use of their corresponding strain–pressure data. These results are quantified in terms of the fiber orientation, defect size and depth, and behavior relative to those of unperturbed pipe sections.

INTRODUCTION

Pipeline integrity and disturbance are generally not monitored due to the lack of any reliable and durable techniques [1]. If a pipeline has a problem, such as cracking, corrosion, tampering, etc., it is usually realized when the output flow is affected or a severe impact has been made on the surrounding environment. No information is available in terms of the type and location of the fault. Obviously, this is an inefficient and potentially costly situation. For example, due to corrosion fatigue cracking, a 28-inch-diameter pipeline ruptured and released about 564,000 gallons of gasoline, on March 9, 2000, in Greenville, Texas, USA, which resulted in a damage/clean-up cost of USD \$18 million [2]. According to the Alberta (Canada) Energy and Utilities Board, there was an abundance of pipeline failures over the past two decades, and internal corrosion is the main cause of pipeline failures [3].

One of the major difficulties of monitoring pipelines stems from the fact that the length of pipeline can be hundreds or thousands of kilometers, buried underground. Conventional conductive sensors have difficulties surviving the environments involved and they have electrical noise problems. Furthermore, conventional sensors are generally point-sensing devices, so that a large number of sensors is required to cover a long pipeline. The subsequent cost and complexity of such a system would thus be impractical. Optical fiber communication cables have proven their capabilities and

survivability in various environmental conditions; hence fiber optic sensors should also be reliable in pipeline applications.

Fiber optic sensor technology has progressed at a rapid pace over the last decade. Many different sensing techniques have been developed to monitor specific parameters [1]. Strain measurement with a distributed Brillouin scattering-based sensor system provides excellent opportunity for the health monitoring of civil structures [4]. It allows measurements to be taken along the entire length of the fiber, rather than at discrete points, by using fiber itself as the sensing medium. One class of Brillouin-based sensors is based on the Brillouin loss technique, whereby two counter-propagating laser beams, a pulse and a CW, exchange energy through an induced acoustic field. When the beat frequency of the laser beams equals the acoustic (Brillouin) frequency, ν_B , the pulsed beam experiences maximum amplification from the CW beam. By measuring the depleted CW beam and scanning the beat frequency of the two lasers, a Brillouin loss spectrum centered about the Brillouin frequency is obtained. The sensing capability of Brillouin scattering arises from the dependence of the Brillouin frequency, ν_B , on the local acoustic velocity and refractive index in glass, which has a linear temperature and strain dependence through [5, 6]

$$\nu_B(T_0, \varepsilon) = C_\varepsilon(\varepsilon - \varepsilon_0) + \nu_{B0}(T_0, \varepsilon_0) \quad (1)$$

$$\nu_B(T, \varepsilon_0) = C_T(T - T_0) + \nu_{B0}(T_0, \varepsilon_0) \quad (2)$$

where C_ε and C_T are the strain and temperature coefficients, and ε_0 and T_0 are the strain and temperature corresponding to a reference Brillouin frequency ν_{B0} . By varying the spatial resolution, it can provide the scale of material strain measurement and structural strain monitoring. Spatial information along the length of the fiber can be obtained through optical time domain analysis (OTDA) by measuring propagation times for light pulses traveling in the fiber. This allows continuous distributions of the strain/temperature to be monitored. This type of sensing has very good potential for structural monitoring. The spatial resolution (gauge length) can be varied according to the application required, even after the fibers have been installed in the structure, by simply altering the length of the light pulse used. These systems offer unmatched flexibility of measurement locations and the ability to monitor a virtually unlimited number of locations simultaneously.

In this work we report our recent experiments of a fiber optic distributed strain and temperature sensor (DSTS) on an internally pressurized 1.8 m long end-capped steel pipe with pre-embedded wall thinning defects. The pre-embedded defects comprising 50% and 60% of inner wall thickness can be discriminated from the corresponding strain measurements with our Brillouin sensor system using 10 cm spatial resolution.

EXPERIMENTAL PROCEDURES

To simulate the structural degradation in pipes, rectangular indentations were entrenched within the inner wall of a steel pipe constructed in the CANMET Materials Technology Laboratory in Ottawa, Ontario, Canada, as seen in Fig. 1. The material specifications of the pipe are listed in Table 1. The pipe was 90% filled with distilled water and pressurized using argon gas. At predetermined locations along its inner wall, structural defects compromising 50-60% of the wall (as shown in Fig. 2) were implanted

to simulate the condition where a corroded pipeline is at a threshold condition of being replaced (50%). When a pipeline corrosion defect occurs, a certain percentage of the inner wall thickness is lost and larger strains appear in the defective region under the constant pressure within the pipe.



Fig. 1. Photograph of the tested steel pipe.

Table 1 Material specifications of the pipe

Poisson's Ratio	Young's Modulus (200 GPa)	Length	Outer diameter	Wall thickness
0.3	30×10^6 psi	183cm	11.4cm	1.1cm

A 30 m acrylate buffered SMF-28 optical fiber was used for monitoring both the environmental temperature conditions and the strain distributions along the pipe. The distribution of defects and sensing fiber installations are shown in Fig. 2; the location and dimensions of the cutouts *A*, *C*, and *D* are tabulated in Table 2; and region *B* constitutes the rest of the unperturbed pipe. To prepare the pipe for fiber installation, sandpaper was used to remove irregularities caused by excess welding and provide a smooth, uniform surface around its circumference. Optical fibers were pre-strained and mounted externally on the pipe to monitor the strain changes at its outer surface, and were secured using a special tape that is easy to be applied to real pipeline monitoring. To avoid signal cross talk and additional noise resulted from fiber overlap, two sets of the fiber were installed sequentially to measure the hoop and longitudinal strains in the configurations shown in Fig. 2. The radial sensing fiber was looped along the pipe, and the axial one was installed longitudinally along the pipe to avoid shear stresses. The temperature of the pipe was monitored using three thermocouples installed at various locations. During measurement trials, the maximum temperature deviation of the pipe was approximately 0.5°C. This temperature information allowed for eventual temperature compensation of the strain measurements. The system is based on the interaction of probe pulse laser and a counter-propagating CW laser for distributed Brillouin sensors at the wavelength of 1552nm.

Brillouin spectrum measurements were acquired every 5cm along 30m fiber every half-hour using 2000 averages, and a 1.0ns pulse width (corresponding to 10cm resolution).

Table 2. Parameters of cutouts (defects)

Cutout	Location (o'clock)	Reduced thickness (%)	Width (cm)	Length (cm)
A	5-7	60	5.3	61
C	7	50	1.3	10
D	5	60	1.3	10

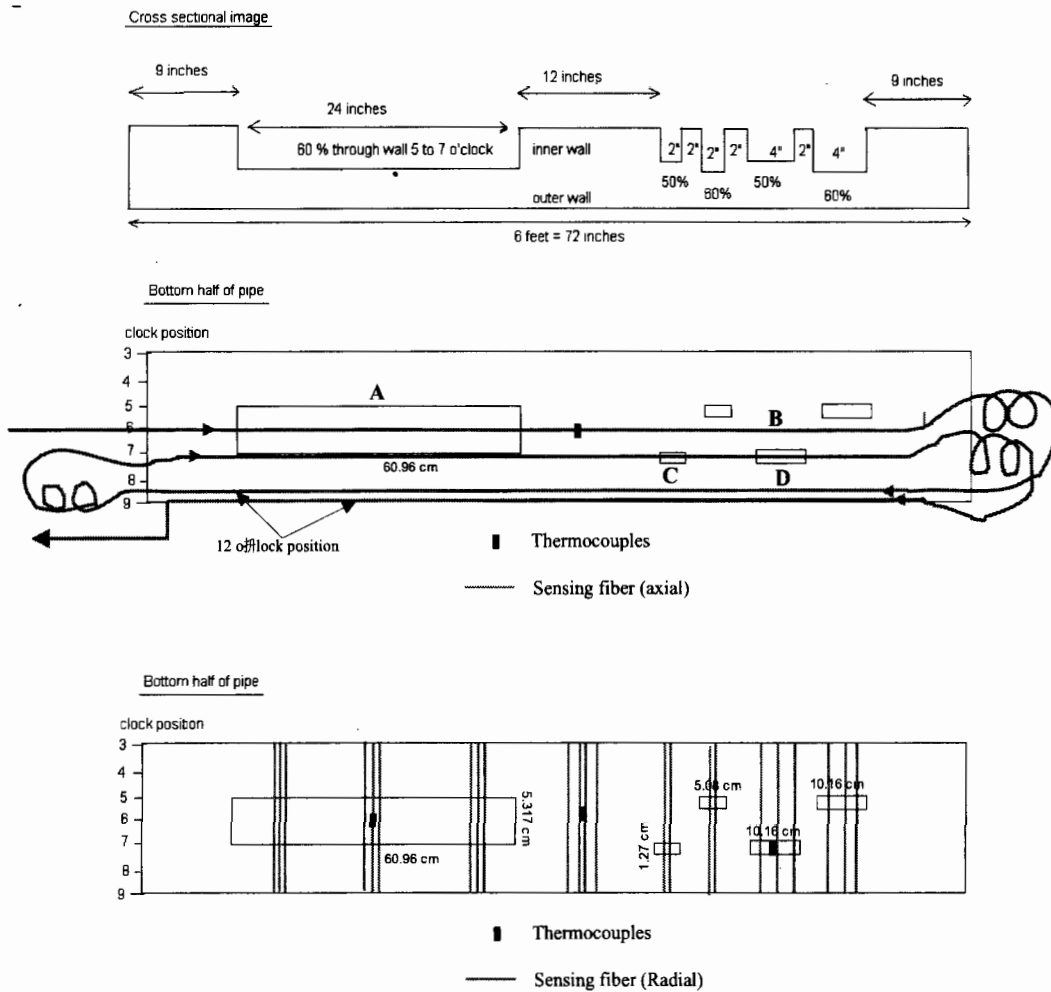


Fig. 2. Schematic diagram of structure defects distribution and sensing fiber installation. For the axial installation of the sensing fiber, A represents the center of 61 cm long cutout from 2 cm to 63 cm. B represents the rest of the unperturbed pipe. C and D indicate a 1-cm wide and 5-cm long defect, and D indicates a 1-cm wide and 10 cm-long defect.

RESULTS AND DISCUSSION

Figs.3 and 4 show typical Brillouin spectra from unperturbed (*B*) and defective (*A*) regions under the internal pressure of 350 psi, respectively.

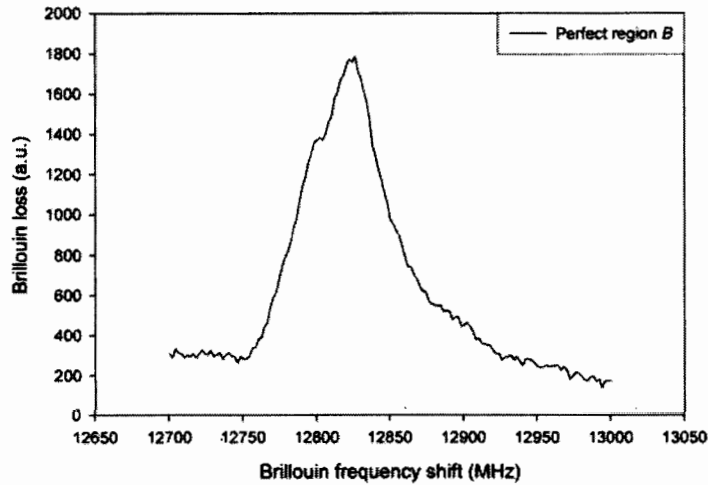


Fig. 3. Brillouin spectrum from unperturbed region (*B*).

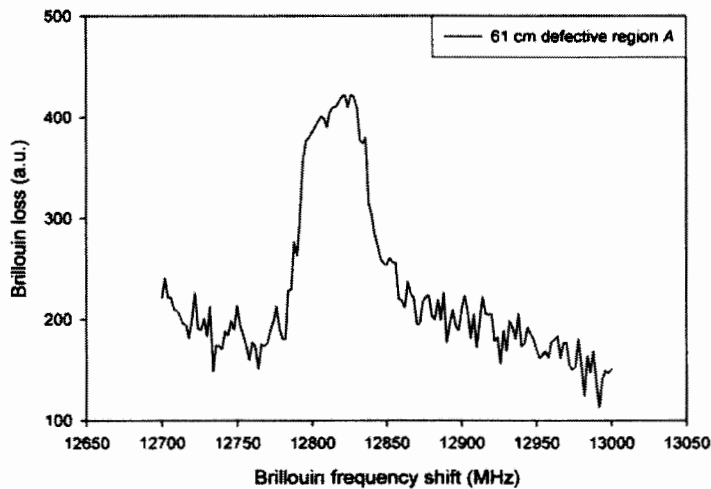


Fig. 4. Brillouin spectrum from defective region (*A*).

Differences in the Brillouin spectra between the perfect region and the defect region are evident on the intensity and strain distributions. These differences can be used to locate defects. The signal strength from defective region is much lower than that from the perfect one due to bending loss caused by bigger deformation of defective region. The measurement is taken at the same reference level for the power.

The strain distribution along longitudinal direction of the pipe under internal pressure 300 psi is presented in Fig. 5. The defect starts at 2cm and ends at 63cm and the rest of the pipe is unperturbed. As expected, the middle of the defective region experienced maximum strain and the minimum strain happened in the middle of the unperturbed region. Because the defective and unperturbed regions located at both sides of

the pipe, the influence of two 42kg weight end caps located at the both ends could not be neglect, which may result in extraordinary strain decrease in the beginning of defective region and increase in the end of unperturbed region.

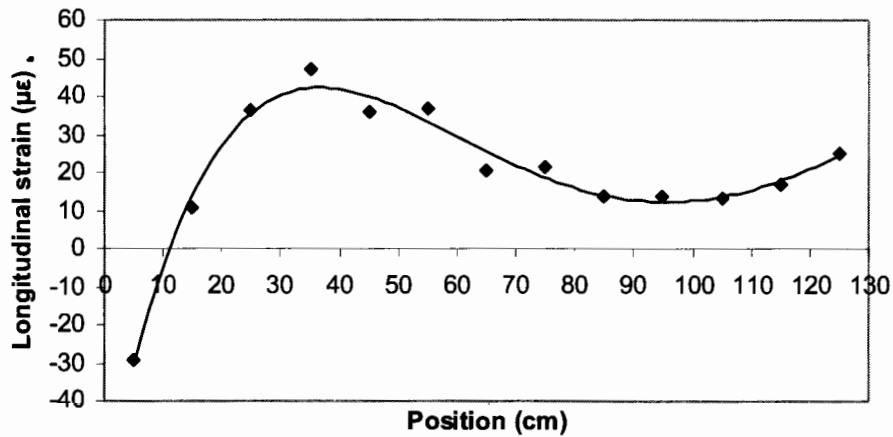


Fig. 5. Longitudinal strain distribution along longitudinal direction of the pipe through defective region (*A*) and unperturbed region (*B*).

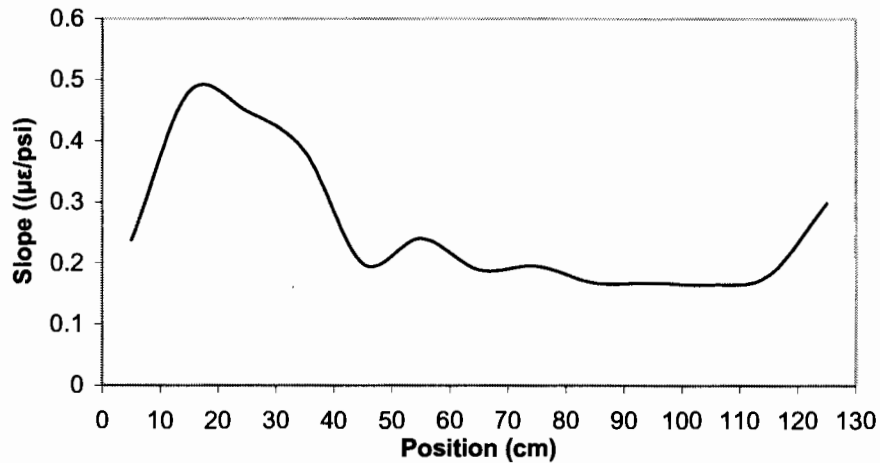


Fig. 6. The longitudinal-strain/internal-pressure along longitudinal direction of the pipe through defective region (*A*) and unperturbed region (*B*).

The slope (strain/pressure) is higher within defective region than within unperturbed region, as shown in Fig. 6. When a uniform pipe is operated within its elastic regime, its strain/pressure curve remains linear. However, erosion or corrosion of the inner pipe wall reduces its thickness, thus increased strain-pressure slope curve occurs within the defective region. The results of strain change with pressure show that the strain-pressure slope at point *A* (the middle of the defect with 60% of inner wall thickness) is greater than at points *D* (the defect with 50% of inner wall thickness) and *B* (the middle of unperturbed region). The slope at point *B* is smallest, indicating that the pre-embedded defects, comprising 50% and 60% of the inner wall thickness, can be discriminated, as shown in Fig. 7.

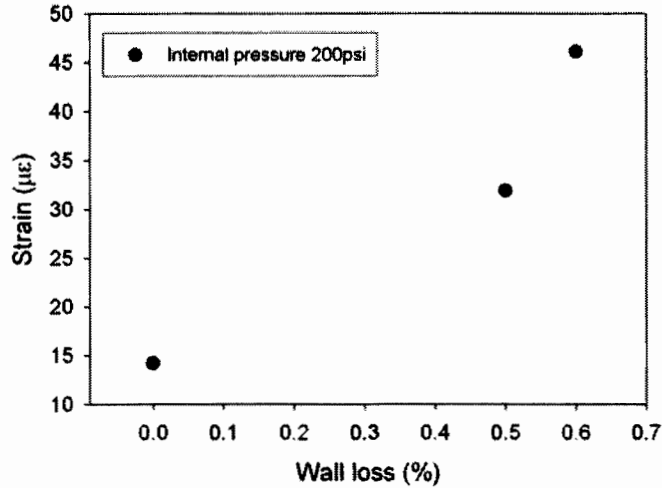


Fig. 7. Comparison of axial strain at defect *A* with 60% wall loss, defect *C* with 50% wall loss, and unperturbed region *B*.

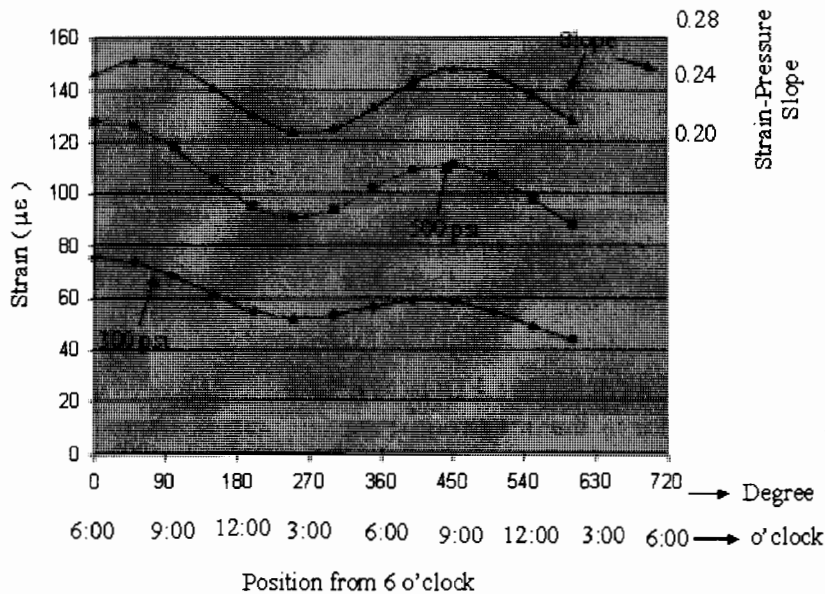


Fig. 8. Hoop strain distribution.

Fig. 8 clearly presents that defective regions can be detected by the Brillouin scattering-based distributed strain and temperature sensor (DSTS) in the hoop configuration: 2 maxima, corresponding to one complete loop, have been observed in the hoop strain distribution of defective region under internal pressures 300 and 500 psi as well as in the strain/pressure slopes of this region at the 6 o'clock position, which matched very well with the cutouts in the pipe. These strain maxima and highest strain/pressure slopes are observed approximately once every 360°.

Fig. 9 displays the comparison of hoop strain around defects *C* with 50% wall loss and *D* with 60% wall loss. Obviously, the thinner pipe experiences greater strain.

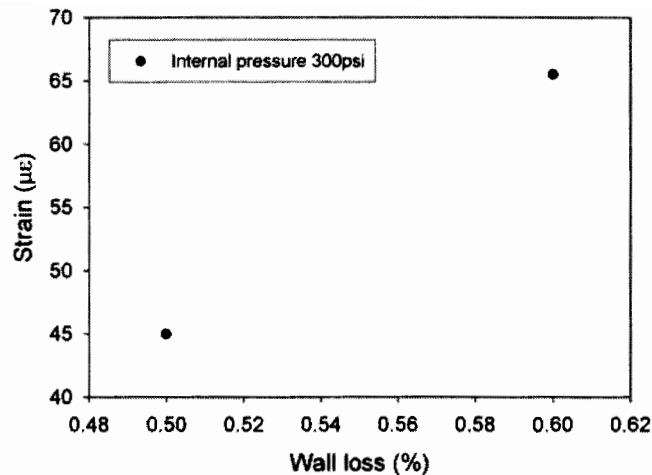


Fig. 9. Comparison of hoop strain around defects *C* with 50% wall loss and *D* with 60% wall loss.

SUMMARY

A distributed Brillouin scattering sensor system was used to measure the longitudinal and hoop strain in an internally pressurized 1.8 m long end-capped steel pipe with wall thinning defects. The pre-embedded defects comprising 50% and 60% of the inner wall have been discriminated from the corresponding strain measurements, showing that fiber optic sensor technology based on distributed Brillouin scattering offers great potential as a “nervous system” for high-performance, cost-effective defect assessment systems.

ACKNOWLEDGEMENTS

The authors would like to thank Gordon Ping Gu and A. Doiron of CANMET Materials Technology Laboratory in Ottawa, Ontario, Canada for associated help, and S. Papavinasam of CANMET Materials Technology Laboratory for useful discussions.

REFERENCES

1. E. Tapanes, “Fibre optic sensing solutions for real-time pipeline integrity monitoring,” Australian Pipeline Industry Association National Convention, 27-30 October 2001, http://www.iceweb.com.au/Newtech/FFT_Pipeline_Integrity_Paper.pdf.
2. Report of the National Transportation Safety Board, “Pipeline accident brief,” (National Transportation Safety Board Headquarters, Washington DC, 2001), <http://www.nts.gov/publicctn/2001/PAB0103.htm>.
3. Report of the Energy and Utilities Board, “Pipeline performance in Alberta 1980-1997,” (Energy and Utilities Board, Calgary, Alberta, Canada, 1998) <http://www.eub.gov.ab.ca/bbs/documents/reports/r98g.pdf>.
4. L. Zou, X. Bao, Y. Wan, and L. Chen, “Coherent probe-pump based Brillouin sensor for centimeter-crack detection,” *Opt. Lett.* **30**, 370–372 (2005).
5. T. Horiguchi, T. Kurashima, and M. Tateda, “Tensile strain dependence of Brillouin frequency shift in silica optical fibers,” *IEEE Photon. Tech. Lett.* **1**, 107-108 (1989).
6. T. Kurashima, T. Horiguchi, and M. Tateda, “Thermal effects on Brillouin frequency shift in jacketed optical silica fibers,” *Appl. Opt.* **29**, 2219-2222 (1990).